1

Theoretical and Experimental Limitations of RoCoF Estimation

J. Gutiérrez-Florensa*, F. Sanniti[†], D. Tedeschi[‡], L. Sigrist[§], Á. Ortega[§] and F. Milano*

* School of Electrical & Electronic Engineering, University College Dublin, Dublin, Ireland [†] Department of Industrial Engineering, University of Padova, Italy [‡] Terna S.p.A., Roma, Italy [§]Institute for Research in Technology, ICAI, Comillas Pontifical University, Madrid, Spain

Abstract—A precise estimation of the Rate of Change of Frequency (RoCoF) is crucial for secure power system operation. In fact, RoCoF is strictly related to the amount of the available physical and/or virtual inertia of the system and the severity of the active power unbalance following a disturbance. For this reason, it is widely exploited in different protection systems, e.g., Anti-Islanding, Under Frequency Load Shedding (UFLS) and wide-area protection systems. The new paradigm of modern power systems, with a low-inertia and converter-based generation assets, is increasing the transient severity, making the frequency and the RoCoF estimation more complex and less precise for the actual devices. This work addresses this issue by proposing a numerically robust approach based on concepts inherited from differential geometry and fluid mechanics. The proposed approach is then tested with high-sampling real experimental measurements and used to develop a faster control logic for a RoCoF-based UFLS control scheme. The proposed approach provides information to protections regarding the nature of the contingency which can be used to improve its response.

Index Terms—differential geometry, fluid mechanics, RoCoF measurement, signal processing, under-frequency load shedding

I. INTRODUCTION

A. Motivation

RoCoF is formally defined as the time derivative of the instantaneous frequency, *i.e.* the second time derivative of the phase angle of a voltage signal [1]. In practical applications, it is computed starting from the estimation of the instantaneous frequency, typically provided by a Phase-Locked Loop (PLL) or from the fundamental frequency estimated by a Phasor Measurement Unit (PMU). Then, the time derivative is computed with the adoption of some filtering and its value is averaged on a rolling time window for a smoother behavior [2]. In addition, for protection schemes, an intentional time delay between the detection and actuation can be used to avoid undesirable trips.

Extended rolling windows are typically adopted to improve the RoCoF estimation by reducing noise, unbalances and distortion, at the expense of the promptness of the relay. On the other hand, a shorter time window improves the responsiveness, but oscillations in the RoCoF estimation, for instance, can lead to undesirable trips.

A recent interpretation of the frequency in the framework of the differential geometry (see [3]) creates the conditions to approach the actual RoCoF computation issues from a novel perspective. In particular, contributions in [4] are especially relevant as they define Quasi Steady-State (QSS) frequency a novel quantity that captures the slowly-varying fundamental

value of frequency - and the time derivative of circulation - a metric that evaluates the physical existence of such frequency. Together, these concepts are here exploited to assess the theoretical and experimental limitations of RoCoF and introduce a novel approach for its estimation.

B. Literature Review

Nowadays, the problem of the RoCoF estimation in power system applications is still an open challenge. Low-inertia systems exhibit higher values of RoCoF during transients and, at the same time, its estimation is harder due to the higher distortion of the electrical quantities [5].

At present, there is no standard approach to compute RoCoF in power systems. Several techniques have been proposed in the last years [6], which can be grouped in two main categories depending on how the frequency is computed: (i) based on instantaneous frequency measurement (provided, *e.g.*, by a PLL or a Finite Impulse Response (FIR) filter [7]), and (ii) based on fundamental frequency measurement (exploiting, *e.g.*, recursive Discrete Fourier Transform (DFT) techniques [8], [9]). As the PLL-based estimation is sensitive to amplitude steps, noise and harmonics, typically the formal estimation of RoCoF is filtered and then averaged on a rolling time window, introducing latency in the estimation [10].

DFT-based techniques can be faster since they elaborate on a phasor measurement, even if they require by definition a given time window for the estimation [9]. These methods are also less sensitive to noise and harmonics but their precision deteriorates especially in the first instant after a disturbance, where the signal distortion is higher [11]. Hence, also in this case a proper averaging window has to be selected, vanishing the promptness of the algorithm [12].

In recent literature, PMU-based techniques for RoCoF estimation have arisen among the others, because of their fast reporting rates and responsiveness, and the wide monitoring ability of the PMU architecture [13]. PMU-based RoCoF estimation techniques do not employ averaging to limit the uncertainty given by noise, distortion, and unbalances. As a consequence, the IEEE has significantly relaxed the RoCoF error requirement from 0.01 Hz/s to 0.4 Hz/s [14]. In practice, this level of uncertainty make the RoCoF estimation useless for typical applications, since values close to 1 Hz/s can already be considered critical for the stability of the system [15]. Several synchrophasor-based algorithms have been compared in [13]

and [12], where it becomes evident that PMUs provide optimal performance in presence of low fluctuations, as typical of interarea oscillations, but their measurement is hampered during fast transient events.

The deployment of RoCoF-based relays is mainly focused on three applications: (i) island detection for distribution networks [16], (ii) protection from Loss of Mains (LoM) of embedded generators [17] and (iii) RoCoF-based UFLS schemes, as part of the power system defense plan of many Transmission System Operators (TSOs) [18]. RoCoF-based UFLS schemes allow improving their responsiveness by anticipating the decision to shed load [19], [20]. The latter application has gained attention in recent years due to the increased penetration of Inverter-Based Resources (IBRs), which is worsening the effects of power disturbances on frequency stability, as recent blackout events have proven [21], [22].

Among several possible topologies of UFLS schemes [23], traditionally based on frequency measurements, semi-adaptive UFLS schemes introduce RoCoF thresholds to trigger the relays in addition to frequency thresholds. For UFLS application, larger absolute RoCoFs values can lead to the following major issues sorted by criticality:

- Frequency collapse before the relays have time to trip;
- Unintentional tripping due to inaccuracy in the measurement of the frequency and/or RoCoF;
- Over extensive Load Schedding (LS) (due to the time delay of activation of the relays).

A trade-off should be found between the promptness of the intervention and the prevention of unintentional trips. In practical applications, often large time windows are chosen, ranging from 500 to 1000 ms [24]. ENTSO-E, *e.g.*, recommends 500 ms as a rolling time window for adequate RoCoF monitoring [2] and recommends also a maximum disconnection time delay [18]. However, to date, recommended criteria for a suitable definition of threshold values and tripping logic are still missing for RoCoF-based UFLS.

C. Contributions

Based on a recent development proposed in [4], the paper further elaborates on the definition of RoCoF by means of QSS frequency and utilizes a metric, namely the time derivative of the circulation, able to determine what parts of the voltage trajectory following a power system transient retain the meaning of a slowly-varying fundamental frequency.

Specific contributions of this work are as follows.

- Derive an expression for the RoCoF based on the derivation of QSS frequency;
- Validate the proposed expression by means of highsampling real-world data provided by the Italian TSO;
- Discuss the impact of the proposed RoCoF estimation on the tripping logic of a semi-adaptive UFLS scheme.

D. Paper Organization

This paper is structured as follows. Section II recalls relevant concepts for the development of the paper and introduces a novel approach for RoCoF estimation. Section III assess a

real-world case scenario to validate the findings in the previous section. Section IV evaluates the potential application of the presented theory in UFLS protections through an specific case study. Section V provides final remarks and discusses practical considerations. Finally, Section VI summarizes the main findings and conclusions of the paper.

II. BACKGROUND AND QSS-BASED ROCOF DEFINITION

Based on recent works (see [3], [4], [25]), we adopt the differential geometry framework to define electrical quantities in direct analogy with fluid mechanics. On this basis, this section recalls the relevant definitions of *QSS frequency* and *time derivative of circulation* from [4], for the developments of the paper, and provides a novel definition of RoCoF based on this theoretical background.

In the context of differential geometry, paper [3] defines geometric frequency multivector, $\hat{\Omega}_{v}$, as an invariant composed by a translation represented by a scalar, ρ_{v} , and an axial vector, ω_{v} , that represents a rotation:

$$\hat{\Omega}_{\boldsymbol{v}} = \rho_{\boldsymbol{v}} + \boldsymbol{\omega}_{\boldsymbol{v}} \,, \tag{1}$$

for:

$$\rho_{\boldsymbol{v}} = \frac{|\boldsymbol{v} \cdot \boldsymbol{v}'|}{|\boldsymbol{v}|^2} \quad ; \quad \boldsymbol{\omega}_{\boldsymbol{v}} = \frac{|\boldsymbol{v} \times \boldsymbol{v}'|}{|\boldsymbol{v}|^2} = \kappa |\boldsymbol{v}| \quad .$$
(2)

Where the latter term closely matches the instantaneous frequency obtained with a conventional PLL as concluded in [26].

In [25], an analogy between geometric frequency and Lagrange's derivative is used to decompose ω_v in different terms with precise physical meanings. These meanings come from the *fundamental theorem of the kinematics of continua* that states that an arbitrary instantaneous state of motion is at each point a uniform velocity of translation, a motion of extension, a shearing motion and a rigid rotation [27]. Among these, for the purposes of this work, the component of interest is the rigid rotation quantified by half the vorticity, w, *i.e.* the curl of voltage $(\nabla \times v)$, as the one that captures the meaning of fundamental frequency.

However, the estimation of vorticity, in this terms, requires to know the relationship between voltages and fluxes which is not possible in practice. For this reason, the work in [4] uses a Cauchy's theorem to define the QSS frequency, ω_{QSS} , as an equivalent quantity of vorticity in fluid mechanics which, for any given period T:

$$\omega_{\text{QSS}} = \frac{1}{T} \oint_{T} \omega_{\boldsymbol{v}} d\tau = \frac{1}{2} \mathbf{w},$$
 (3)

for any given period T where the second identity is the result of Cauchy's theorem, when no torsion is assumed. The quantity $\omega_{\rm QSS}$ thus conceptually bridges instantaneous and Fourier's frequency by retaining the slowly-varying fundamental frequency meaning while being valid not only during ideal balanced stationary conditions.

The election of period T is not trivial and is determined by the aforementioned Cauchy's theorem applicability condition. Cauchy's theorem is valid for regular curves that fulfill:

$$\kappa_T = \oint_{s_T} \kappa \, ds = \oint_T \kappa |\mathbf{v}| \, d\tau = \oint_T |\mathbf{\omega}_{\mathbf{v}}| \, d\tau = 2\pi \,, \quad (4)$$

where κ_T and s_T are the total curvature and arc length respectively. Note that this is, in fact, the necessary condition, for a space curve, to describe a Jordan's curve, *i.e.* a simple closed curve [28]. Thus, we define the period as:

$$T = \inf \left\{ t : t > t_0, \int_{t_0}^{t+t_0} |\omega_{\upsilon}| d\tau = 2\pi \right\}.$$
 (5)

Period, by means of (5), is defined through the voltage trajectory as the time it takes, for a given initial time t_0 , to close the described curve. Alternatively, if the trajectory does not draw a closed curve, period and, consequently, frequency cannot be defined.

In summary, estimation of QSS frequency requires to assume that the trajectory describes a Jordan curve. For this reason, [4] defines a metric, namely time derivative of circulation, Γ' , independent from condition (5), to determine wether this assumption is satisfied. Voltage trajectory describes a closed curve and, hence, QSS frequency retains the fundamental frequency value of the signal if:

$$\Gamma' = \oint_T (|\boldsymbol{v}|^2)' d\tau = 0, \qquad (6)$$

whereas if $\Gamma' \neq 0$, voltage trajectory is not closed and QSS frequency measurement lacks of physical meaning associated with periodicity. This condition is derived from the analog definition of circulation in fluid mechanics ($\Gamma = \oint_T |\boldsymbol{v}|^2 d\tau$) and the application of Kelvin's circulation theorem.

As in practice it is not realistic to expect to obtain exactly zero from (6) due to measurement and numerical errors, we compare Γ' to a threshold, ϵ , that allows us to discriminate if the non-zero outcome comes from unavoidable practical errors or due to the loss of periodicity. Hence, at any instant t, the voltage is assumed to be periodic and $\omega_{\rm QSS}$ to be defined if:

$$|\Gamma'| < \epsilon \,. \tag{7}$$

Then, RoCoF can be obtained as the time derivative of QSS frequency subject to condition (7):

RoCoF =
$$\omega'_{OSS}$$
, if $|\Gamma'| \le \epsilon$. (8)

However, in real-world applications, RoCoF calculation involving a derivative of $\omega_{\rm QSS}$ can be prone to noise and numerical issues. For this reason, in practice, RoCoF is normally estimated as an average value of a mobile window, within a time span, Δt_w , to filter out oscillations, distortions, etc. [24]. However, such window might include "wrongly" measured frequency values such as spikes during the transient.

In this work, we propose a novel RoCoF estimation approach that derives the rate of change of QSS frequency and does not take into account the time intervals where frequency lacks physical meaning, namely, condition (7) is not satisfied. To do so, we first introduce a *tout function*, $\mathcal{T}(\Gamma')$, that substantially implements a conditional boolean value:

$$\mathscr{T}(\Gamma') = \frac{\operatorname{sign}(\epsilon - |\Gamma'|) + 1}{2}, \tag{9}$$

that returns a 1 if condition (7) is satisfied and 0 otherwise.

We can then define the average RoCoF estimation as:

$$\overline{\text{RoCoF}} = \frac{1}{\Delta \tilde{t}_w} \int_{t-\Delta t_w}^t \boldsymbol{\omega}_{\text{QSS}}' \mathcal{T}(\Gamma') d\tau$$
 (10)

where $\Delta \tilde{t}_w = \int_{t-\Delta t_w}^t \mathscr{T}(\Gamma') \, d\tau$. The main feature of this RoCoF estimation approach is that periods where frequency is not defined do not contribute to the calculation of the average. Moreover, the tout function provides information of the nature of any sudden frequency variation, which can be used to adapt the average time window for a faster estimation without loss of precision.

III. VALIDATION THROUGH MEASUREMENTS

In this section, expression (10) is applied to high-sampling-rate measurements in order to compare it with the conventional RoCoF computation from instantaneous frequency. The available recordings, with a sample rate of 5kHz, were provided by the Italian TSO (Terna S.p.A.) and are related to a transformer energisation during a power system restoration test performed on a region of the Italian Transmission Network¹. The measured voltage time response related to the event is shown in Fig. 1.

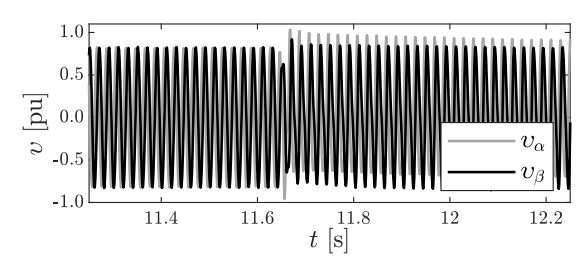


Fig. 1: Measurements of the normalized voltage measurements during the transformer energisation event in the $\alpha\beta\gamma$ frame.

Instantaneous frequency estimation, ω_{υ} , from PLL has been filtered through a first-order Butterworth filter. Both instantaneous and QSS frequency results are shown in Fig. 2. Results show that the latter filters out the oscillations under stationary conditions while damping the spikes in the transient. This behavior is consistent with the findings in [4].

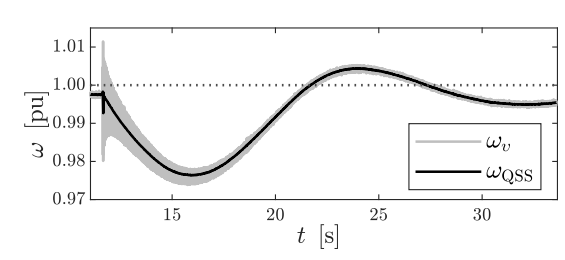


Fig. 2: Instantaneous frequency, ω_v , and QSS frequency, $\omega_{\rm QSS}$, results of the transformer energisation case study.

The immediate consequence of these results is that the formal estimation of the RoCoF by means of the QSS frequency in (8) is less sensitive to noise than conventional instantaneous frequency estimation, as shown in Fig. 3.

¹Note that frequency and RoCoF relays have been disabled for the purpose of the test as the transformer energisation leads to significant RoCoF deviations during the first instants due to the small size of the network.

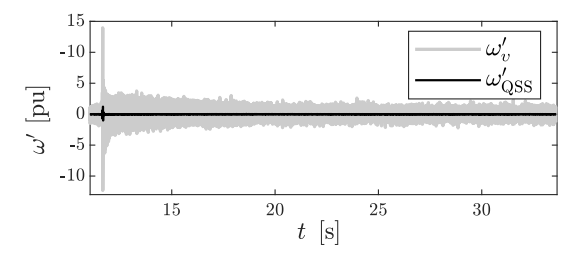


Fig. 3: Time derivative of instantaneous and QSS frequency, ω_v' and ω_{QSS}' respectively, of the transformer energisation case study.

As previously stated, a rolling average can be applied to the formal estimation of the RoCoF and therefore, the estimation in (8) is compared to the one proposed in (10), requiring satisfying the circulation condition. With this in mind, we first assess the time derivative of circulation. We set the threshold $\epsilon=0.05$ by considering the noise in the measurement under stationary conditions. Results show that condition (7) is not satisfied during the energization transient (see Fig. 4) and, hence, frequency (and thus RoCoF) estimation lacks of physical meaning.

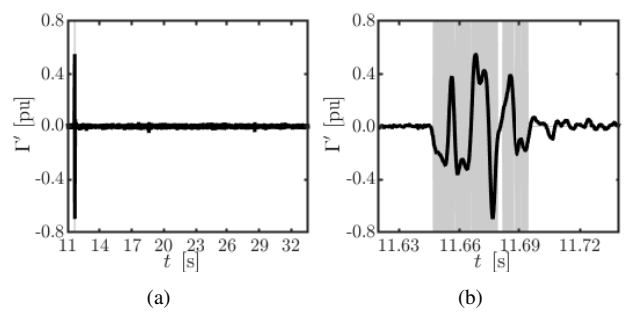


Fig. 4: Overview of time derivative circulation, Γ' , results of the transformer energization case study (a), and detailed view of the results under the event (b). Periods where condition (7) is not satisfied are gray shadowed.

By knowing the instants of satisfying the circulation condition, we finally estimate the RoCoF as an average value of a rolling window of $\Delta t_w = 500$ ms, as recommended by ENTSO-E (see [2]), for both instantaneous frequency measurement and the proposed approach in (10). Figure 5 depicts the results. Red dashed lines represents RoCoF values of ± 1 Hz/s, namely, the minimum values considered potentially critical for the stability of the system [15].

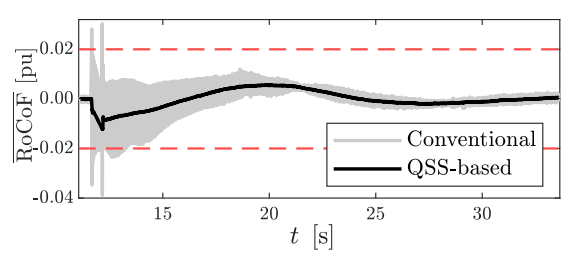


Fig. 5: RoCoF estimation as an average of time derivative of instantaneous frequency (Conventional) and by definition in (10) (QSS-based) for $\Delta t_w = 500$ ms. Red-dotted line represents a realistic threshold for system stability control.

In the first instants after the disturbance, the RoCoF computed by the instantaneous frequency exceeds the critical

values, whereas the QSS-based RoCoF stays within them (as it should be in this case). Moreover, the spikes during the transient might lead to the wrong conclusion that frequency is increasing, whereas the proposed approach is capable of smoothing that response by providing a more accurate estimation of the RoCoF as the time derivative of frequency.

The inherently smoother response of the proposed approach allows us to shorten the size of the rolling time window, Δt_w , of the RoCoF estimation. Conventional estimation requires longer time windows to ensure noise and transient spikes are averaged out. Estimation by means of QSS frequency, excluding periods in which frequency and, consequently, RoCoF are not defined, permits a less restrictive methodology.

To support this conclusion, Fig. 6 plots the results of conventional RoCoF estimation for $\Delta t_w = 500$ ms and by means of (10) with 50% shorter rolling window. Results prove that, although reducing the averaging interval, the QSS based RoCoF estimation is less affected by noise and still remains within the normal operating range.

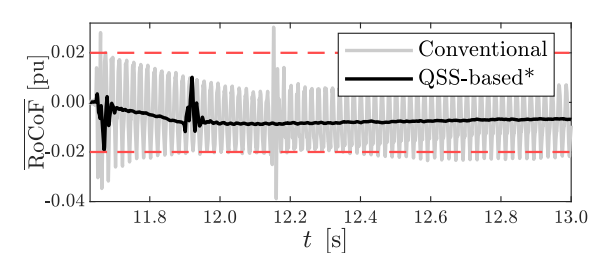


Fig. 6: Detailed view of RoCoF estimation as an average of time derivative of instantaneous frequency for $\Delta t_w = 500$ ms (Conventional) and by definition in (10) with a reduced time window, $\Delta t_w = 250$ ms (QSS-based*). Red-dotted line represents a realistic threshold for system stability control.

IV. APPLYING OSS-BASED ROCOF TO UFLS

In this Section, we present a potential application aimed to improve the RoCoF estimation of RoCoF-based protection relays in UFLS schemes. For the purpose of this study, a semi-realistic scenario is set up starting from the IEEE 39-bus benchmark system, considering the dynamics of the lines, to simulate a large outage and the subsequent activation of a two-step RoCoF-based UFLS scheme. The UFLS scheme has been implemented according to the simulation platform presented in [29], which can represent a benchmark for testing the effectiveness of RoCoF estimation in power system applications.

The IEEE 39-bus system has been modified to emulate a low-inertia system. In particular, a set of IBRs are added at every generation bus. The IBR model employed and its primary controllers are described in [30]. At generation buses, the power share of IBRs is imposed through the parameter $\gamma \in [0,1]$, which scales the capacity of both synchronous machines and IBRs to ensure that the total generation capacity $S_{\rm n}$ remains constant:

$$S_{\rm n}^{\rm IBR} = S_{\rm n} \gamma \quad ; \quad S_{\rm n}^{\rm Syn} = S_{\rm n} (1 - \gamma) \quad , \qquad (11)$$

where $S^{\rm IBR}$ and $S^{\rm Syn}$ refer to the apparent power delivered by IBR and synchronous resources respectively.

Inertia constants, H, power rates, S_n , and synchronous and transient reactances, x_d , $x_{d'}$, x_q , $x_{q'}$ of each synchronous machine are scaled accordingly. IBR models and controllers utilized in this case study include current limiters and anti wind-up limiters. With these aforementioned assumptions, the modified 39-bus system is configured as a low-inertia system.

A two-step semi-adaptive UFLS scheme has been applied to all buses where a load is connected. Figure 7 shows the diagram of the UFLS scheme acting on the k^{th} -load. We assume here that a PLL computes the instantaneous frequency, ω_k , starting from the bus voltage v_k , which is then passed through a low-pass filter and a washout filter by the RoCoF block to compute $\overline{\text{RoCoF}}_k$. The way in which $\overline{\text{RoCoF}}_k$ is computed can be different if we consider the enhancement given by the derivation of Γ' —see (10).

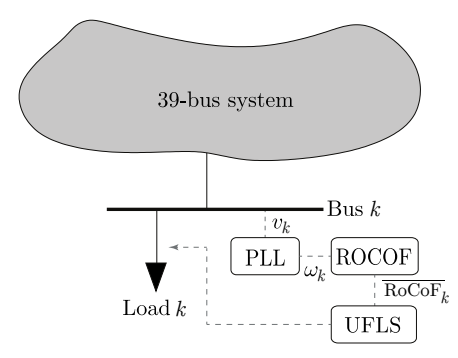


Fig. 7: Diagram of the UFLS scheme for each load bus k of the IEEE 39-bus modified system.

Figure 8 details the two tripping logic schemes implemented in the UFLS block adopted for the simulations. $t_{\rm trigger}$ refers to the time when a transient event occurs, $t_{d\omega}$ to the time when the rolling window detects a RoCoF value exceeding a threshold and $t_{\rm trip}$ to the time when the protection trips.

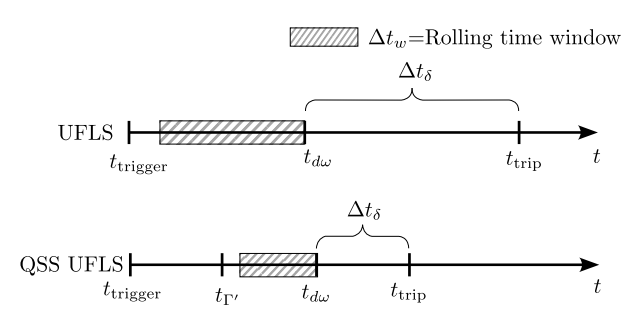


Fig. 8: Tripping logic of the implemented UFLS schemes.

We consider a conventional tripping logic, labeled as UFLS, characterized by a large rolling window, Δt_w , and a large time delay, Δt_{δ} , according to the recommendations given in [2], [18] and the simulation performed in [29]. Then, we propose a tripping logic based on the considerations expounded in the previous sections, named QSS UFLS, where we are able to exclude from the rolling time window Δt_w the first instants after a trigger event where the frequency has no physical meaning associated with periodicity, until time $t_{\Gamma'}$. Since we are sure that, starting from that instant, what we are measuring is a signal with a defined period, we can afford to shorten Δt_w .

In this way, the relay issuing is faster but without the risk of unintentional tripping.

Regarding the UFLS tripping scheme, it consists of two RoCoF thresholds, $d\omega_1$ and $d\omega_2$ which command the disconnection of two LS portions, namely ΔLS_1 and ΔLS_2 respectively. Fig. 9 shows the tripping scheme adopted for the simulations. In this specific scenario, the purely frequency thresholds are not implemented on purpose, since the aim is to analyze the effect of RoCoF measurements on the UFLS scheme and so on the dynamic performance of the system.

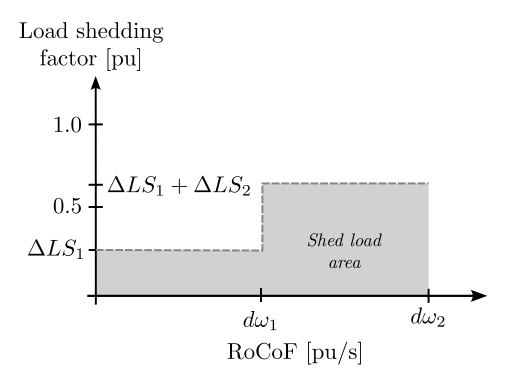


Fig. 9: Tripping thresholds of the implemented UFLS schemes.

A large generation outage, involving both synchronous generators and IBR installed on buses 1, 2, 8, 10 is simulated, for a total of 2.44 GW of power outage. The sum of the two thresholds of all UFLS disconnects a total of 2.43 GW of load, balancing the initial outage. Parameter values utilised in the simulations are shown in Table I.

TABLE I: Data setting for the UFLS scheme of Fig. 7.

Param.	Description	UFLS	QSS
			UFLS
K_i	[-] PLL integral gain	0.03	0.03
K_p	[-] PLL proportional gain	0.2	0.2
T_w	[s] frequency LP filter time const.	0.01	0.01
T_r	[s] RoCoF washout filter time const.	0.01	0.01
Δt_w	[s] time window for RoCoF est.	0.5	0.25
ϵ	[pu] circulation threshold	-	0.05
$\Delta t_{\Gamma'}$	[s] Initial time span where $ \Gamma' > \epsilon$	0.0	0.023
$d\omega_1$	[pu/s] 1st UFLS threshold	0.012	0.012
$d\omega_2$	[pu/s] 2 nd UFLS threshold	0.024	0.024
$\Delta t_{\delta,1}$	[s] trip delay for 1 st UFLS threshold	0.2	0.2
$\Delta t_{\delta,2}$	[s] trip delay for 2^{nd} UFLS threshold	0.2	0.2
ΔLS_1	[pu] Load shed by the 1^{st} UFLS threshold	0.2	0.2
ΔLS_2	[pu] Load shed by the 2^{nd} UFLS threshold	0.2	0.2

A. UFLS ROCOF performance results

The results of the simulations are depicted in Fig. 10. The three curves represent the frequency of the Center of Inertia (CoI) for three different simulations:

- (i) **NO UFLS**: the UFLS is disabled.
- (ii) UFLS: the RoCoF-based UFLS scheme is enabled.
- (iii) QSS UFLS: the QSS RoCoF-based UFLS scheme is enabled.

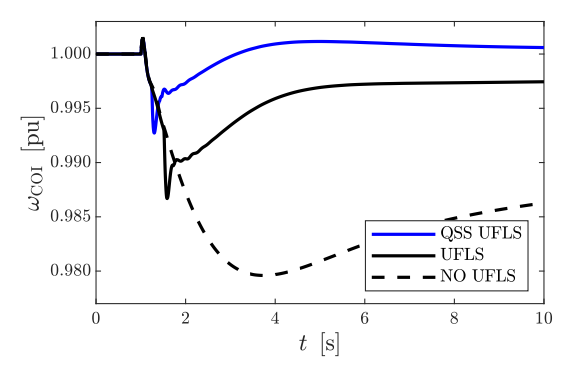


Fig. 10: CoI frequency response for different UFLS schemes with the specific parameters from Table I.

UFLS protection scheme, effectively, improves the system response in terms of frequency stability. The QSS RoCoF-based UFLS sheds more load and earlier than the conventional UFLS logic. This is because on the one hand RoCoFs vary among the buses and on the other hand, the conventional UFLS estimation is slower and at some load buses does not exceed the thresholds due to the larger window. This behavior can be seen in Figs. 11 and 12 that show, respectively, the time derivative of frequency and average RoCoF estimations at bus 20. This case illustrates that the accuracy and speed of RoCoF estimation could be critical for UFLS after all if the conventional estimation and logic falls short.

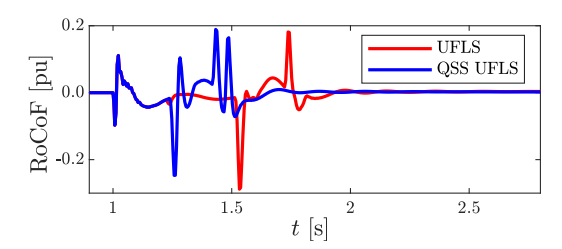


Fig. 11: RoCoF estimation results, at bus 20, by means of frequency time derivative for conv. and QSS UFLS schemes.

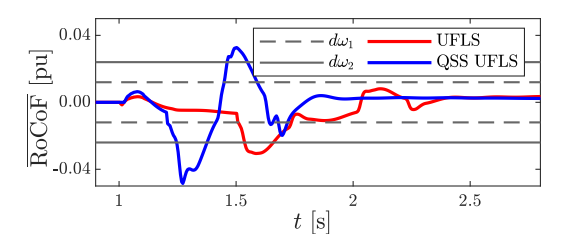


Fig. 12: RoCoF estimation results, at bus 20, by means of the average of frequency time derivative for conv. and QSS UFLS schemes. Threshold values, $d\omega_1$ and $d\omega_2$, are represented by a black line and a black dotted line respectively.

V. REMARKS

A. On the Practical Implications

When estimating the RoCoF, choosing a suitable time window involves a trade-off between measurement accuracy and response promptness. Although an optimal window length may exist within this balance, UFLS devices lack knowledge

of the nature of the threshold violation event. For this reason, typically prefixed conventional values are used.

By delaying the RoCoF computation, the optimal time window can be shortened. However, delaying too much can cause an insufficient or entirely absent response. Hence, the choice of a time delay is nontrivial and should not be established beforehand, as it depends on the nature of the contingency.

The proposed omission of RoCoF values that do not fulfill condition (7) right after the contingency, inherently introduces a delay that affects the UFLS response. The introduction of such delay, by means of Γ' , ensures that the RoCoF estimation is delayed properly; only non-representative values of RoCoF are omitted. Consequently, averaging time window and tripping delays can be reduced, thereby improving the protection response. Moreover, as demonstrated in Section III, the estimation of the RoCoF by means of QSS frequency is less affected by noise than conventional estimations based on instantaneous frequency, thus enabling faster estimation without compromising accuracy.

B. On the election of threshold ϵ

The need of defining ϵ comes from potential numerical errors and the discrete nature of the measurements. If ϵ is too restrictive (too small), the tout function, $\mathcal{T}(\Gamma')$, might continuously detect noise or estimation imperfections as transient events that lack periodicity, being the edge case equivalent, in the practical application, to not applying the UFLS protection. Conversely, if ϵ is too permissive (too large), $\mathcal{T}(\Gamma')$ might not detect such events and frequency response will be equivalent as conventional RoCoF estimation-based UFLS protection response. From this perspective, conventional UFLS schemes can be seen as a specific case of the QSS-based scheme with a, *de facto*, over-dimensioned threshold for the system requirements.

The choice of ϵ is guided by experimental observation. As shown in [4], transient events that lack periodicity represent an abrupt change of Γ' , making the discernment of events, with respect to their nature, quite evident. To support this statement we plot, in Fig 13, the initial time delay, $\Delta t_{\Gamma'}$, with respect of different ϵ values, of the practical application case study.

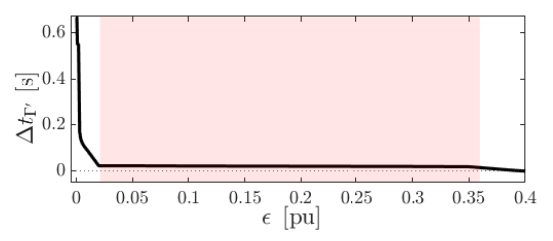


Fig. 13: Initial time span where condition (7) is not satisfied with respect of different threshold, ϵ , values. Range of QSS RoCoF-based UFLS optimal performance is red-shadowed.

Within the edge cases, the vast majority of the range of possible ϵ values falls in a plateau where the delay, $\Delta t_{\Gamma'}$, does not change. Following the findings in [4], the ϵ value, of a specific model, should be chosen only based on the sampling time of the discrete data. From the experience obtained from

real-world data, we recommend to evaluate ϵ considering measurements taken in stationary conditions and set a quite over-dimensioned value, e.g. one order of magnitude higher.

VI. CONCLUSIONS

This paper discusses theoretical and experimental limitations of the RoCoF computation and proposes a novel definition of RoCoF, which is more compliant with the challenges issued by the actual structure of the power system. Thanks to the definition of the QSS frequency and the time derivative of the circulation, the time intervals where the frequency has no physical meaning are excluded from the moving average of the classical RoCoF computation.

This definition shows a significant improvement in the RoCoF estimation when applied to real-world measurement, helping to avoid possible unintentional tripping of RoCoF-based relays during highly-distorted transient events. Moreover, if applied to a RoCoF-based UFLS scheme, robust frequency estimation, by means of $\omega_{\rm QSS}$, and information from Γ' can be used to adapt and shorten the typical rolling window and time delay before the issuing of the relay, speeding up the frequency restoration and decreasing the absolute value of the frequency nadir.

REFERENCES

- "IEEE/IEC International Standard Measuring relays and protection equipment - Part 118-1: Synchrophasor for power systems - Measurements," pp. 1–78, 2018.
- [2] ENTSO-E, "Rate of change of frequency (RoCoF) withstand capability, ENTSO-E guidance document for national implementation for network codes on grid connection," Brussels, Blegium, Tech. Rep., 2018.
- [3] F. Milano, "A Geometrical Interpretation of Frequency," *IEEE Trans. Power Syst.*, vol. 37, no. 1, pp. 816–819, 2022.
- [4] J. Gutiérrez-Florensa, Á. Ortega, L. Sigrist, and F. Milano, "Quasi steady-state frequency," *IEEE Trans. on Circuits and Systems I: Regular Papers, early access*, pp. 1–13, 2025.
- [5] A. Riepnieks and H. Kirkham, "Rate of change of frequency measurement," in *Int. Scientific Conference on Power and Electrical Engineering* of Riga Technical University (RTUCON), 2016, pp. 1–5.
- [6] X. Deng et al., "Review of RoCoF Estimation Techniques for Low-Inertia Power Systems," Energies, vol. 16, no. 9, 2023.
- [7] R. Ferrero, P. A. Pegoraro, and S. Toscani, "Proposals and analysis of space vector-based phase-locked-loop techniques for synchrophasor, frequency, and ROCOF measurements," *IEEE Trans. on Instr. and Meas.*, vol. 69, no. 5, pp. 2345–2354, 2020.
- [8] M. Bertocco et al., "Compressive Sensing of a Taylor-Fourier Multifrequency Model for Synchrophasor Estimation," *IEEE Trans. on Instr. and Meas.*, vol. 64, no. 12, pp. 3274–3283, 2015.
- [9] A. K. Singh and B. C. Pal, "Rate of Change of Frequency Estimation for Power Systems Using Interpolated DFT and Kalman Filter," *IEEE Transactions on Power Systems*, vol. 34, no. 4, pp. 2509–2517, 2019.
- [10] P. S. Wright et al., "Field Measurement of Frequency and ROCOF in the Presence of Phase Steps," *IEEE Trans. on Instr. and Meas.*, vol. 68, no. 6, pp. 1688–1695, 2019.
- [11] Y. Zuo, G. Frigo, A. Derviškadić, and M. Paolone, "Impact of Synchrophasor Estimation Algorithms in ROCOF-Based Under-Frequency Load-Shedding," *IEEE Trans. on Power Systems*, vol. 35, no. 2, pp. 1305–1316, 2020.
- [12] G. Rietveld, P. S. Wright, and A. J. Roscoe, "Reliable Rate-of-Change-of-Frequency Measurements: Use Cases and Test Conditions," *IEEE Trans. on Instr. and Meas.*, vol. 69, no. 9, pp. 6657–6666, 2020.
- [13] G. Frigo, A. Derviškadić, Y. Zuo, and M. Paolone, "PMU-Based ROCOF Measurements: Uncertainty Limits and Metrological Significance in Power System Applications," *IEEE Trans. on Instr. and Meas.*, vol. 68, no. 10, pp. 3810–3822, 2019.
- [14] "IEEE standard for synchrophasor measurements for power systems amendment 1: Modification of selected performance requirements," pp. 1–25, 2014.

- [15] ENTSO-E RG-CE System Protection & Dynamics Sub Group, "Frequency Stability Evaluation Criteria for the Synchronous Zone of Continental Europe," Brussels, Belgium, Tech. Rep., 2016.
- [16] P. Gupta, R. S. Bhatia, and D. K. Jain, "Active ROCOF Relay for Islanding Detection," *IEEE Trans. Power Del.*, vol. 32, no. 1, pp. 420– 429, 2017.
- [17] D. M. Laverty, R. J. Best, and D. J. Morrow, "Loss-of-mains protection system by application of phasor measurement unit technology with experimentally assessed threshold settings," *IET Generation, Transmission & Distribution*, vol. 9, no. 2, pp. 146–153, 2015.
- [18] ENTSO-E System Protection and Dynamics Sub Group, "Technical Background and Recommendations for Defence Plans in the Continental Europe Synchronous Area," Brussels, Belgium, Tech. Rep., 2010.
- [19] M. Sun, G. Liu, M. Popov, V. Terzija, and S. Azizi, "Underfrequency Load Shedding Using Locally Estimated RoCoF of the Center of Inertia," *IEEE Trans. Power Syst.*, vol. 36, no. 5, pp. 4212–4222, 2021.
- [20] P. Kundur et al., "Power system stability," Power system stability and control, vol. 10, no. 1, pp. 7–1, 2007.
- [21] ENTSO-E. (2025) 28 April Blackout. [Online]. Available: https://www.entsoe.eu/publications/blackout/28-april-2025-iberian-blackout/
- [22] G. Lemos, A. Melgar, M. Torres, and M. Rios. State of emergency declared after blackout plunges most of Chile into darkness. [Online]. Available: edition.cnn.com/2025/02/25/americas/chile-blackout-14-regions-intl-latam
- [23] U. Rudez and R. Mihalic, "Wams-based underfrequency load shedding with short-term frequency prediction," *IEEE Trans. Power Del.*, vol. 31, no. 4, pp. 1912–1920, 2016.
- [24] ENTSO-E, "Inertia and Rate of Change of Frequency (RoCoF)," ENTSO-E, Brussels, Belgium, Tech. Rep. v17, 2020.
- [25] F. Milano, "Equivalence Between Geometric Frequency and Lagrange Derivative," *IEEE Trans. Circuits Syst. I*, vol. 72, no. 9, pp. 4800–4809, 2025.
- [26] F. Milano et al., "Using differential geometry to revisit the paradoxes of the instantaneous frequency," *IEEE Open Access Journal of Power* and Energy, vol. 9, pp. 501–513, 2022.
- [27] C. Truesdell, The Kinematics of Vorticity. Indiana, US: Indiana University Press, 1954.
- [28] J. J. Stoker, Differential Geometry. John Wiley & Sons, Ltd, 1969.
- [29] A. Derviškadić, Y. Zuo, G. Frigo, and M. Paolone, "Under Frequency Load Shedding based on PMU Estimates of Frequency and ROCOF," in *IEEE ISGT-Europe*, 2018, pp. 1–6.
- [30] G. Tzounas and F. Milano, "Improving the frequency response of DERs through voltage feedback," in *IEEE PES General Meeting*, 2021, pp. 1–5